Research Article / Review Article FUPRE JOURNAL 8(3): 175-187 (2024)

FUPRE Journal

of

Scientific and Industrial Research

ISSN: 2579-1184(Print) ISSN: 2578-1129 (Online)

http://fupre.edu.ng/journal

Synthesis, Characterisation, and Antibacterial Activities of Cu(I) Complexes Bearing (N^N) Bidentate Schiff Bases having Triphenylphosphine Ancillary Ligand.

ODULAJA, S. O. [1,*], ***ADELEKE, A. A.*** [1], ***AMOLEGBE, S. A.*** [2], ***SANYAOLU, N. O.*** [1], ***YUSSUF, S. T.*** [1], ***HASHIMI, A. M.*** [1]

[1] *Department of Chemical Sciences, Olabisi Onabanjo University, Ago-Iwoye, Nigeria.*
[2] *Department of Chemistry, College of Physical Sciences, Federal University of Agriculture, Abeokuta, Nigeria*

ARTICLE INFO

Received: 20/02/2023
Accepted: 20/05/2024

Keywords

Ancillary, Chemotherapeutic, Pyridine carboxaldehyde, Schiff base, triphenylphosphine

ABSTRACT

This work synthesized new biologically active Cu(I) complexes 1-5, obtained from the reaction of Cu(I) nitrate with different bidentate pyridinyl Schiff base ligands (E)1-(pyridin-2-yl)-N-(p-tolyl)methanimine L1, (E)-1-(pyridin-2-yl)-N-(o-tolyl)methanimine L2, (E)-N-isopropyl-1-(pyridine-2-yl)methanimine L3, (E)-N-mesityl-(pyridinyl)methanimine L4 and (E)-N-(2,6-dimethylphenyl)-1-(pyridine-2-yl)methanimine L5, with PPh_3 ancillary ligand. The metal complexes with general formula $[Cu\ L(PPh_3)_2]NO_3$, were characterised by FT-IR, UV-Vis, NMR and MS, X-ray crystallography and elemental analysis. The antibacterial activities against Staphylococcus aureus (SA), Escherichia coli (EC), Klebsiella pneumonia and Pseudomonas aeruginosa (PA) were investigated using agar well diffusion method with ofloxacin as reference. UV-Visible spectra and FT-IR result showed bathochromic shift in the imino (C=N) frequencies in the complexes confirming coordination to the metal centre. Single crystals obtained in complexes 2, 3, 5 revealed orthorhombic crystal systems having Tau (τ4) values in the range 0.73 - 0.87 depicting distorted tetrahedral geometries. Coordination to the metal center was bidentate for all the ligands via the pyridinyl N and imine N in conjunction with two triphenylphosphine P in the N^N^P^P fashion in complexes 2, 3, and N^N^P^O fashion in complex 5. The antibacterial activities revealed that all the complexes exhibited better antibacterial activities relative to their parent ligands and PPh_3. The study found out that the newly synthesized complexes have better antibacterial performances hence make the metal complexes potential chemotherapeutic agents in drug design.

1. INTRODUCTION

Combatting infectious and life-threatening diseases remains a challenge due to the preponderance of multidrug resistance and re-emerging infectious diseases (Morse, 2001.). Antimicrobial resistance (AMR) has remained an emerging problem worldwide, posing a global health threat. The once effective antimicrobial drugs against different microorganisms are no longer effective due to indiscriminate overuse of antimicrobial drugs, inappropriate drug choices, inadequate dosage and poor adherence to treatment instructions (Marston et al., 2016.) Consequently, there is an urgent need to introduce effective antimicrobial agents. The coordination

*Corresponding author, e-mail: olufemi.odulaja@oouagoiwoye.edu.ng
DIO

chemistry of copper complexes of Schiff base has been a subject of extensive research over the years (Andruh, 2015.). In spite of reported activity of copper complexes of Schiff bases, the structure and biological activities of these metal complexes of Schiff bases in conjunction with ancillary ligands still has more to be researched into (Ribeiro et al., 2017.). The stabilization of copper(I) by hemilabile ligands such as triphenylphosphines, forms some of the earliest studies of coordination chemistry (Simkhovich, 2000.). Subsequent work has demonstrated a diversity of structures and stoichiometries (Karp et al., 2020; Shabbir et al., 2016.). The complexation of N'N bidentate Schiff base ligands with triphenylphosphine complexes may bring about several structural motifs, hence varied biological activity (Dharmaraj et al., 2001; Viswanathamurthi et al., 2005.). Numerous bidentate Schiff base complexes of copper(I) have been reported, the present work focuses on biological activity in the presence of ancillary ligands. Thus, as part of recent investigations of the triphenylphosphine complexes (Griebel et al., 2020.), we report the synthesis of Cu(I) and pyridinyl Schiff base and triphenylphosphine ligands with high antibacterial activity.

2.0 EXPERIMENTAL

2.1 Synthesis of ligands L1 – L5

The ligands were prepared by the condensation reaction of 2-pyridinecarboxaldehyde with different substituted anilines (*o*- toluidine, **L2**; isopropylamine, **L3**; and 2, 6-dimethylaniline, **L5**) in anhydrous methanol. In the FT-IR spectra of ligands **L1**–**L5**, the disappearance of carbonyl stretching bands ν(C=O) and appearance of the imine ν(C=N) absorption band between 1624 and 1644 cm^{-1}, suggests the synthesis of the proposed Schiff base ligands (Adeleke, 2023, 2020; Njogu et al., 2017.).

2.2 Synthesis of copper precursor [Cu(I) $(PPh_3)_2$]

Bis-(triphenylphosphine) copper(I) nitrate has previously been synthesized, however in this study, a slightly modified literature procedure was employed (Lobana et al., 1989.) in the *Bis*-(triphenylphosphine) copper(I) nitrate synthesis. Triphenylphosphine (0.524 g, 2 mmol) was added to ethanol in a 250 mL round bottomed flask and stirred continuously for 30 minutes at 40 °C until a clear solution was obtained. Copper (I) nitrate (0.13 g, 1 mmol) was added slowly, and the reaction mixture refluxed for 1 h. The round bottomed flask and the reaction mixture was transferred and quenched in an ice bath for 30 min and thereafter filtered. A pale blue air–stable crystalline product was formed and allowed to dry overnight.

2.3 Synthesis of copper(I) complexes 1–5

Copper complexes **1–5** (Scheme 1) were synthesized by dropwise addition of 10 mL methanolic solutions of each of **L1 – L5** (1 mmol) to solutions (*ca.* 10 mL) of $[Cu(PPh_3)_2]NO_3$ (1.0 mmol, ca. 0.65 g) in dichloromethane under constant stirring at 25 °C for 12 h. The precipitates were first isolated from the solution by evaporating the solvents at reduced pressure using a rotary evaporator. The complexes obtained were recrystallized by dissolving the precipitates in dichloromethane. Single crystals suitable for an X-ray diffraction were obtained *via* a solvent layering process using diethyl ether onto the dichloromethane solutions of **1-5** at room temperature.

2.4 X-ray crystallography

Crystal evaluation and data collection of **2, 3** and **5** were recorded on a Bruker Apex Duo diffractometer equipped with an Oxford Instruments Cryojet operating at 100(2) K and an Incoatec microsource operating at 30 W power. The data were collected with Mo Kα (λ = 0.71073 Å) radiation at a crystal-to-detector distance of 50 mm using omega and phi scans. The structures of **2, 3** and **5** were solved by the direct method using the SHELXS (Sheldrick, 2015.) program and refined. The visual crystal structure information was performed using

ORTEP-3 (Farrugia, 2012.), system software. Non hydrogen atoms were first refined isotropically and then by anisotropic refinement with a full-matrix least-squares method based on F^2 using SHELXL (Sheldrick, 2008.). All hydrogen atoms were positioned geometrically, allowed to ride on their parent atoms, and refined isotropically.

2.5 Antimicrobial study

In vitro antibacterial study of complexes **1–5** were carried out using the Agar well diffusion method. The Mueller Hilton agar plate was inoculated by spreading a known volume of test organism inoculum (0.5 McFaland Standard) over the entire agar plate. Then a hole with a diameter of 6mm was punched aseptically with a sterile cock borer which was filled with the samples at varied concentrations. Compound concentrations were calculated in terms of percentage (100%, 50% and 25%). 0.1ml of each sample was injected into the wells. Then, agar plates were incubated at suitable conditions for the test organisms. Clear zones around the well showed antimicrobial activities of the samples (Cross et al., 2018.).

3.0 RESULTS AND DISCUSSION

3.1 UV-visible absorption

A summary of physicochemical parameters of the complexes **1-5**, the absorption wavelengths, assignments are shown in Table 3.1. Electronic absorption spectra recorded in 10^{-3} M DMSO at room temperature in the UV-visible region of the free ligands **L1–L5** and their corresponding Cu(I) complexes **1–5** are presented in Figure 3.1a,b. The absorption spectra of all ligands **L1-L5** showed two major absorption bands in the UV region between 230 – 245 nm and 310 – 335 nm attributed to n–π * and π–π * transitions respectively. The first (230 – 245 nm) is compatible with benzene ring absorption while the second (310 – 335 nm) depicts the imino group absorption band. In the Cu(I) complexes **1** and **2** arising from ligand **L1** and **L2** absorption spectra (Figure 1a), only one absorption band in the UV region of between 318–325 nm was observed in the complexes and attributed to π–π * transitions accompanied with a barthochromic shift associated with decrease in energy at the excited state upon coordination to copper. Complex **5** however, showed one major absorption band between 260 – 270 nm with a characteristic hyperchromic shift associated with shortening of wavelength. Generally, each of the five ligands showed two absorption bands (230–245 nm and 310–335 nm) whereas only one absorption band (310 – 335 nm) were observed in the complexes except complex **4** that shows a shoulder at 240 nm, the disappearance of absorption bands in the UV region of 230 – 245 nm in the Cu(I) complexes is attributed to metal coordination (Zheng et al., 2022b.).

3.2 FT-IR Spectroscopy

Coordination of **L1**–**L5** to the Cu(I) centres were monitored by comparing the FT-IR spectrum of the free ligands with their respective complexes. Table 3.2 shows the Summary of the absorption bands attributed to signature functional groups of the ligands and complexes (Figure **S**6-10). The absorption bands at 1624–1644 cm^{-1} in the FT-IR spectra of **L1**, **L3**, **L4** and **L5**

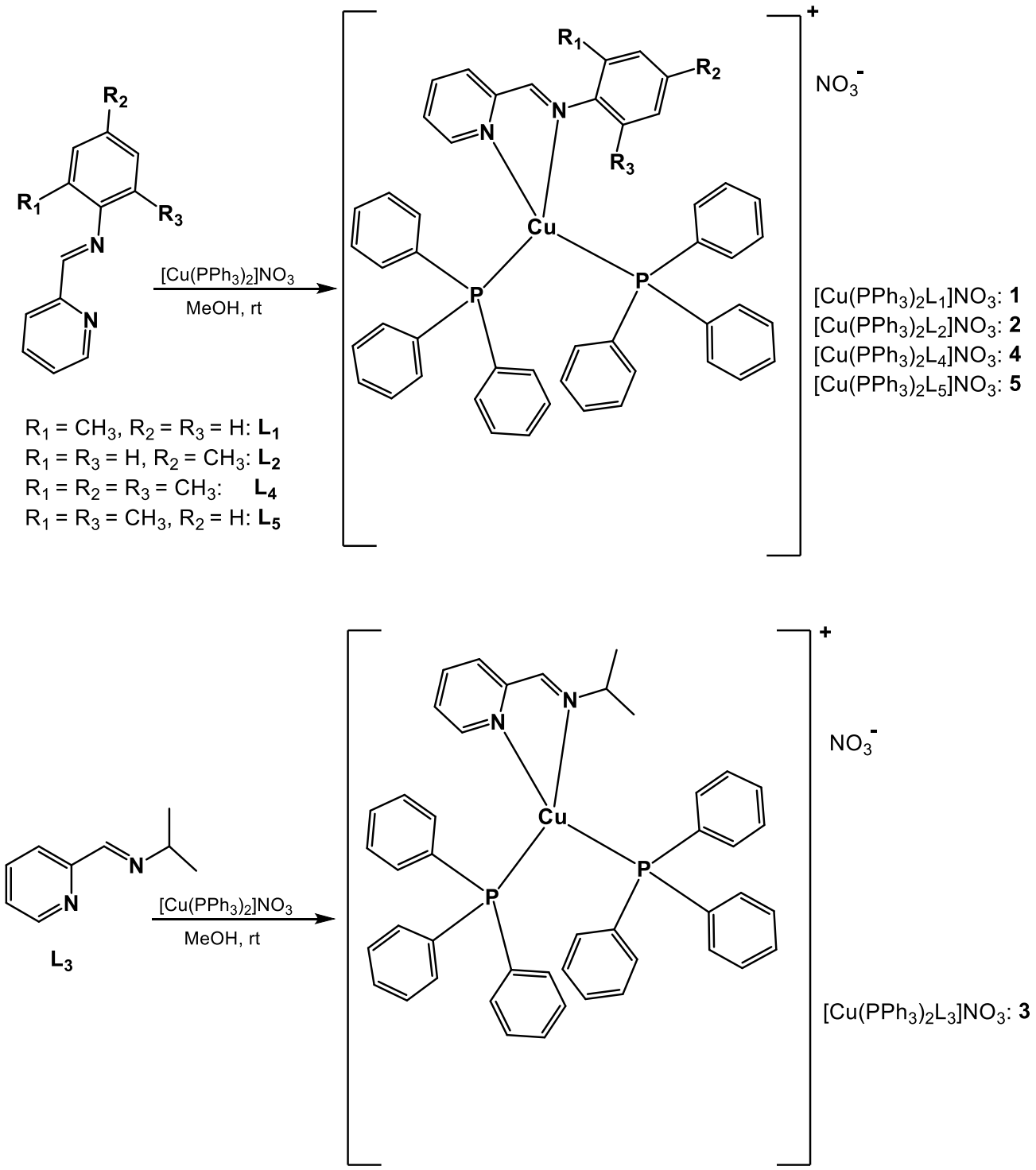

Scheme 2.1: Synthesis of complexes **1–5** under constant magnetic stirring in anhydrous methanol

Table 3.1: Physicochemical data and UV-Visble absorption values of complexes 1-5 with assignments

Complex	Molecular formula	Colour	Yield	Melting point (°C)	Wavelength	Assignment	Elemental Analysis (Calcd.)		
							C	H	N
1	$C_{49}H_{42}CuN_3O_3P_2$	Yellow	60	241	330	$\pi \rightarrow \pi^*$	70.10(69.54)	5.38(5.00)	5.18(4.96)
2				253	335				17(4.96)
3					273				35(5.36)
4				267	240				03(4.81)
5					278 274				22(7.03)

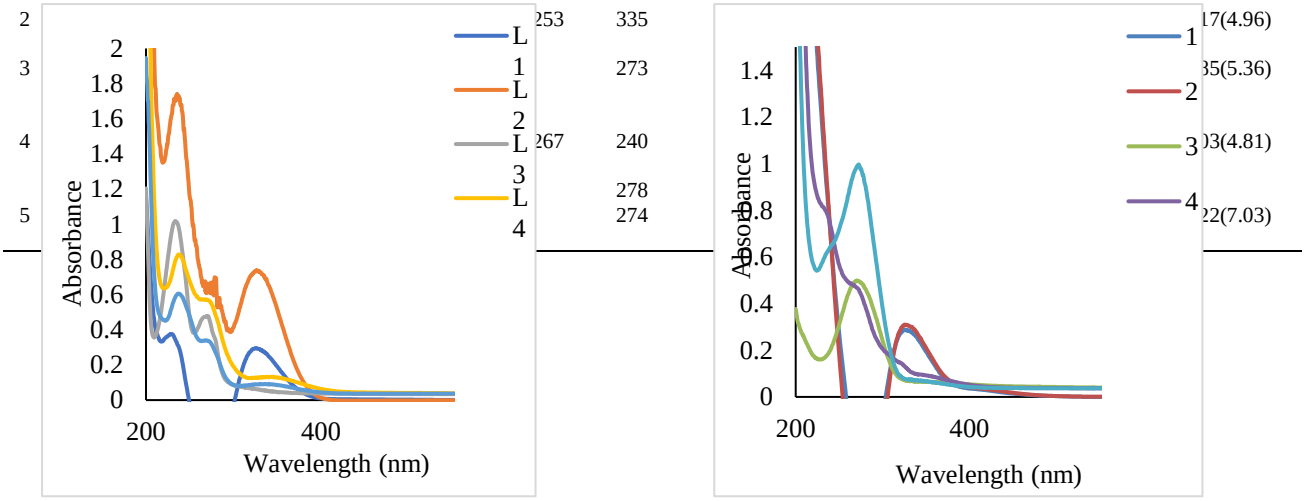

(a) **(c)**

Figure 3.1: UV-Visible data of ligands L1-L5(a), and UV-Visible data of Cu (I)complexes 1-5 (b)

ligands associated with the imino bond stretching frequencies showed bathochromic shift to lower frequencies 1622 and 1636 cm^{-1} band upon coordination to Cu(I), in complexes **1, 3, 4** and **5** with the lone exception of complex **2,** whose vibrational frequency showed hypsochromic shift to higher frequencies from 1624 to 1635 cm^{-1} upon coordination. The absorption bands associated with the pyridinyl ring in the range 1565–1584 cm^{-1} in the spectra of **L1**–**L5** shifted to higher wavenumbers in the range 1585–1588 cm^{-1} upon coordination in the complexes **1-5**. All ligands **L1-L5** were coordinated to Cu(I) via the imine and pyridinyl nitrogen donor atoms. The strong sharp bands observed between 1270 and 1340 cm^{-1} in all the complexes is attributed to the anionic functional group NO_3^-. Moreover, the presence of sharp bands at 1440-1460 cm^{-1} in all the complexes is suggestive of the presence of triphenylphosphine (Ramachandran et al., 2012.)

Table 3.2: FT-IR Spectra data of imino and pyridinyl functional group of ligands **L1-L5** and their respective Cu(I) complexes **1-5**

Ligand(Complex)	ν(C=N) cm^{-1}	Δν	ν(py—N) cm^{-1}
L1(1)	1624(1622)	2	1565(1587)
L2(2)	1624(1635)	11	1565(1585)
L3(3)	1644(1636)	8	1586(1587)
L4(4)	1637(1619)	18	1584(1587)
L5(5)	1640(1628)	12	1585(1588)

3.3. ^{1}H NMR

Table 3.3, presents the summary of the chemical shifts observed in the ligands and the complexes as shown in (Figures **S**11-20). The ^{1}H- NMR spectra of nearest neighbouring proton to the pyridine donor atoms in ligands **L1**–**L5** were compared to that of complexes 1–**5**, and a glaring downfield shift in the protons around the pyridinyl N atoms was observed in each case. Conversely a noticeable upfield shift was observed in the azomethine alpha protons peak in the spectra of complexes relative to the free ligands. For instance in the ^{1}H- NMR of **L1** and **L2**, the azomethine proton appeared as a singlet at 8.59 and 8.49 ppm respectively (Figure **S**11 and **S**12) and consequent upon complexation in **1** and **2**, the azomethine proton blue-shifted to a singlet at 8.91 and 8.86 ppm resulting in a chemical shift difference Δδ of 0.32 and 0.37 ppm respectively (Figure **S**16 and **S**17). In **L3** the azomethine proton appeared as a singlet at 8.30 ppm while that of its complex **3** appeared as a singlet at 8.91 ppm depicting an upfield shift. In complex **4,** the imino proton chemical shift was observed as a singlet at 8.59 ppm whereas, its ligand **L4** appeared as a singlet at 8.28 ppm. Similar trends of upfield shifts were observed in all the complexes **1-5**. The highest difference in chemical shift between ligand and complex was observed in ligand **L3** and complex **3** with a Δδ of 0.61, this may be due to the aliphatic aniline derivative in the ligand. In contrast, the smallest observed chemical shift difference (Δδ) of 0.31 was recorded between ligand **L4** and complex **4,** asides all the ligands containing aromatic anilines derivatives had chemical shift difference Δδ ranging from approximately 0.31-0.37. These shifts buttressed the evidence of coordination of the ligands to the Cu(I) centre via the imino N and pyridinyl N in all the complexes which are in tandem with reports on similar pyridinyl complexes.

Table 3.3: ^{1}H, ^{13}C and ^{31}P NMR chemical shifts in ligands **L1-L5** and complexes **1-5**

	^{1}H NMR (ppm)				^{13}C NMR (ppm)				^{31}P NMR
Lig.(Comp.)	δ_H (C=N)	$\Delta\delta_H$	δ_H (py—N)	$\Delta\delta_H$	δ_C (C=N)	$\Delta\delta_C$	δ_C (py—N)	$\Delta\delta_C$	$\delta_P(PPh_3)$
L1(1)	8.59 (8.91)	0.32	8.70 (8.30)	0.4	160.24 (164.53)	4.06	154.65 (150.29)	4.36	2.51
L2(2)	8.49(8.86)	0.37	8.70(8.60)	0.10	160.40(164.46)	4.06	154.68(150.74)	3.94	2.34
L3(3)	8.30(8.91)	0.61	8.60(8.34)	0.26	159.48(160.58)	0.10	154.72(150.70)	3.98	27.05 1.95
L4(4)	8.28(8.59)	0.31	8.72(8.36)	0.36	164.57(166.85)	2.28	154.89(150.26)	4.63	2.08
L5(5)	8.30(8.81)	0.51	8.70(8.32)	0.38	163.59(164.45)	0.86	153.73(150.74)	2.99	4.68

3.4 Mass spectroscopy

The mass spectra of **1–5** in methanol were all obtained in the positive ion mode and unequivocally confirmed coordination of ligands **L1** - **L5** to Cu(I) centres in all the five complexes (Figure S36-40**)**. All the spectra showed signals, which correspond to species containing the ligands, the triphenylphosphine co-ligand together with the copper ion. The peak at m/z = 521 for complexes **1** and **2** arising from **[Cu(L1)PPh$_3$)]$^+$** and **[Cu(L2)PPh$_3$)]$^+$**, m/z = 521 consequent upon dissociation of one triphenylphosphine co-ligand moiety from the coordination sphere (Vijayan et al., 2014.). For complex **3**, the expected isotopic mass distribution of 474.01 was observed at peak m/z = 473.15 (100%) attributed to **[Cu(L3)PPh$_3$)]$^+$**. Complexes **4** and **5** showed peaks at 549.18 and 535.13 respectively with 100% abundance attributed

to **[Cu(L4)PPh$_3$)]$^+$** and **[Cu(L5)PPh$_3$)]$^+$** respectively. All the peaks are also in tandem with the expected isotopic mass distribution for the respective complexes in the positive ion mode.

3.5. Solid-state structures of complexes 2, 3 and 5

The crystallographic data and structure refinement for complexes **2**, **3** and **5** are shown in Table 3.4, Figure 3.2a,b and c however shows the molecular structures and ORTEP diagrams. The asymmetric unit of **2** and **3** consist of one (*E*)-1-(pyridin-2-yl)-*N*-(*o*-tolyl)methanimine and (*E*)-*N*-isopropyl-1-(pyridine-2-yl)methanimine molecule respectively. In each of complexes **2** and **3**, the copper(I) is coordinated to a pyridine N and imine N in a bidentate manner with copper(I) further coordinated to two triphenylphosphine P completing a distorted tetrahedral coordination while nitrate anion is outside the coordinating sphere. The angles around the copper(I) center range from 79.68(11)° and 122.29(9)°. The asymmetric unit of **5** consists of one (*E*)-*N*-(2,6-dimethylphenyl)-1-(pyridine-2-yl)methanimine ligand, one triphenylphosphine, one copper(I) and a nitrate. The Cu(I) is coordinated to two nitrogens from pyridine N and imine N in a bidentate fashion like in **2** and **3,** but only one triphenylphosphine moiety via P and the nitrate in this case inside the coordination sphere in the (N'N'P'O) fashion resulting in a distorted tetrahedral geometry . The acute angles around the Cu(I) centers are (Npy—Cu—Nim) ranging from 79.68(11)° to 80.65.(6)° and obtuse (Npy—Cu—P1, Nim—Cu—P2 and P1—Cu—P2) angles ranging between 107.48(8) and 133.69(3)° for all the complexes (Table 5). Geometry index for four coordinates complex τ_4 (Eq. (3)) was used to determine the complexes geometry.

$$\frac{360 - (\alpha + \beta)}{141°} \qquad (3)$$

The τ_4 values are 0.87, 0.86 and 0.73 for complexes **2**, **3** and **5** respectively which fits in distorted tetrahedral geometry in accordance with those of the literature (Adeleke et al., 2021; Adeleke, 2021; Njogu et al., 2017; Njogu, 2018; Schnödt et al., 2011; Zheng et al., 2022a.). All the complexes are unsymmetrical structurally and, therefore, belong to the **6** point group (Yang et al., 2007.). In complexes **2**, **3** and **5**, the angles of the pyridine N and imine N bond around the Cu(I) center are acute angles 79.68(11)°, 80.12(5)° and (80.65(5)° respectively are not significantly different, however in **2** and **3**, the pyridine N coordinates to the Cu(I) center to complete a distorted tetrahedral geometry with Npy—Cu—P1 being 107.48(8)° and 108.73(3)° respectively while the bond angle is significantly larger in **5** (Npy—Cu—P1 = 133.69(3)°) confirming anion coordination and the influence on geometries around Cu(I). Evidence of distorted tetrahedral geometry of **5** is further supported by the Nim—Cu—O angle being 98.95(4)° which is substantially smaller than the Nim— Cu—P2 bond angle 112.48(9)° and 114.59(3)° in **2** and **3** in that order (Pettinari et al., 2016; Sun, 2013.). A structural comparison of complexes **2**, **3** and **5** clearly shows that increasing steric effects can lead to the formation of different structural motifs. For complexes **2** and **3** arising from ligand **L2** and **L3** respectively, the *para* and *ortho* methyl substituent on the aniline ring allow coordination of two triphenylphosphine P, the pyridine N, and imine N to the copper center, whereas, for complex **5** arising from ligand **L5** instead of forming a similar N'N'P'P mononuclear Cu(I) complex, the bulkier dimethyl substituent on ligand **L5** apparently forces the nitrate O to coordinate to copper(I) center and form a mononuclear N'N'P'O complex **5**, suggesting the steric effect posed by the bulkier dimethyl substituent of the pyridinyl Schiff base on second triphenylphosphine moiety. Thus complex **5**, [Cu(L5)PPh$_3$)NO$_3$] exhibits distorted tetrahedral structure in (Figure 2c). To our knowledge, only two examples in

which a Cu(I) ion possesses the same N'N'O'P coordination environment have been reported (Karlin, 1987; Santini et al., 2002.). The Cu–P bond distance (2.1737(4) A°) in complex **5** is in tandem with these two examples and comparable to others in previously reported Cu(I)–PPh_3 (Adeleke et al., 2021.)

Table 3.4: Crystallographic data and structure refinement for complexes **2, 3** and **5**

	2	**3**	**5**
Empirical formula	$C_{49}H_{42}CuN_3O_3P_2$	$C_{45}H_{42}CuN_3O_3P_2$	$C_{32}H_{29}CuN_3O_3P$
Formular weight	846.33	798.31	598.10
Temperature:	100 K	101 K	100 K
Wavelength	1.54178	1.54178	1.54178
Crystal system	Orthorhombic	Monoclinic	Monoclinic
Space group	$P2_1$	$P2_{1/c}$	$P2_{1/n}$
a (Å)	13.5101(4)	12.8096(3)	8.7303(3)
b (Å)	14.3061(5	14.7190(4)	13.5090(5)
c (Å)	21.4035(7)	20.2506(5	24.3501(9)
α (°)	90	90	90
β (°)	90	95.414(1)	93.080(2)
ϒ (°)	90	90	90
Volume ($Å^3$)	4136.8(2)	3801.11(17)	2867.65(18)
Z	4	4	4
ρ_{calc} g/cm^3	1.359	1.395	1.385
μ/mm^{-1}	1.846	1.971	1.908
F(000)	1760.0	1664.0	1240.0
θ range for data collection/°	7.432to 146.54	6.932to 134.78	7.27 to 134.52
Goodness-of-fit on F^2	1.040	1.066	1.040
Crystal size/mm^3	0.402 x 0.280 x 0.101	0.405 × 0.275 × 0.085	0.191 × 0.125 × 0.11
Index ranges	16 ≤ h ≤ 16 -17 ≤ k ≤ 17, -25 ≤ l ≤ 26	-15 ≤ h ≤ 15, -17 ≤ k ≤ 17, -24 ≤ l ≤ 24	-10 ≤ h ≤ 10, -16 ≤ k ≤ 16, -29 ≤ l ≤ 29
Reflections collected	56790	85712	42648
Independent reflections	7994[R_{int}=0.0826, Rσ =0.0581]	6843[R_{int}=0.0345, Rσ =0.0145]	5139[R_{int}=0.0328, Rσ =0.018]
Data completeness	0.998	1.000	0.998
Largestdiff.peak/hole/e $Å^{-3}$	0.23/-0.22	0.30/-0.38	0.42/-0.33

(a) **(b)**

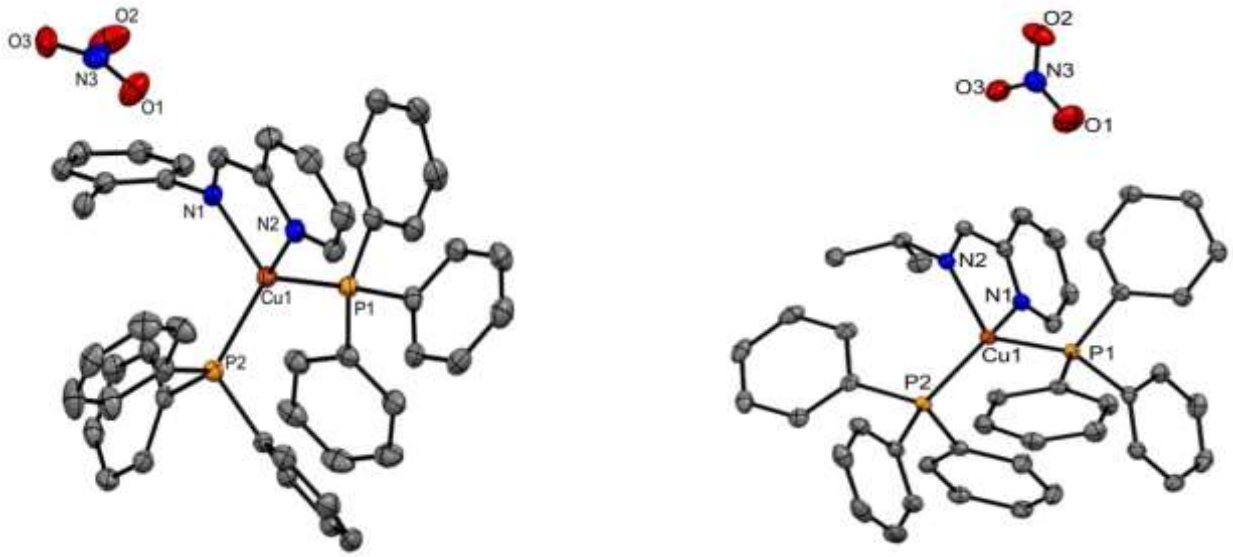

(a) ***(b)***

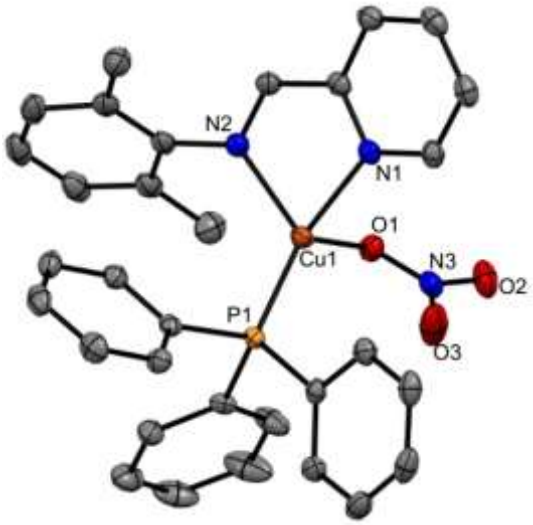

(c)

Figure 3.1: ORTEP diagrams showing complexes (a) **2**, (b) **3**, (c) **5** (Hydrogen atoms have been omitted for clarity.

3.6 In vitro antibacterial study

Ligands **L1**–**L5**, the precursor and complexes **1**–**5**, along with ofloxacin (used as a standard), were screened for antimicrobial activity against one Gram-positive bacteria, *S. aureus*, and three Gram-negative bacteria, *E. coli*, *K. pneumoniae*, and *P. aeruginosa*. The inhibitory concentrations given in figure 3.5 indicated that complexes **1**–**5** generally had better antibacterial activity compared to **L1**–**L5**, indicating that complexation to Cu(I) enhanced the antimicrobial properties of **L1**–**L5**. It is suspected that the complexes have increased ability to penetrate the bacterial cell membranes due to enhanced lipophilicity of the complexes. In such a process, the lipid layer of the bacterial cells gets infiltrated, and the respiration process gets destroyed, thereby inhibiting bacterial growth which often times results in cell apoptosis.(Raj et al., 2017.). All the complexes **1–5**, were generally more active against *S. aureus*, the least active complex **3** showed an activity greater than two-fold the activity of the most active ligand **L3**. It is also observable that complexes **2** and **5** were more active than ofloxacin standard. Gram-negative bacteria usually have a thinner cell membrane making accessibility and permeation easier. All the complexes showed significantly high activity against *E. coli* except complex **3** which was inactive and the inhibitory activity of 28 exhibited by **2** was also higher than the activity of the standard. Each of the complexes **1–5** showed high activity against at least two bacterial species, these complexes possess either one or two triphenylphosphine moiety in addition to *para* or *ortho* methyl substituents on the phenyl ring. The high lipophilic nature of the triphenylphosphine moiety (Raman et al., 2009.) in the complexes is assumed to be responsible for their high activities. In **3**, the aliphatic moiety could have limited its activity (Oladipo & Mocktar, 2019.) as the electron donating group would lead to low lipophilicity but the presence of two triphenylphosphine moiety must have enhanced the activity. Complex **5**, which has only one triphenyl phosphine moiety, was also active against S. aureus and *E. coli* with a value of 23 and 25 respectively but weakly active against *K. pneumoniae*. The weak activity could be as result of influence of the only triphenylphosphine which is reduced by the electron withdrawing nitrate coordinated to the metal center through *O* atom.

4. CONCLUSION

We have synthesized and structurally characterized copper(I) complexes of pyridinyl Schiff bases with triphenylphosphine as ancillary ligand. Molecular structures of all the complexes reveal bidentate coordination of the Schiff base to the copper(I) center, while two molecules of triphenylphosphine are equally coordinated to the copper(I) center in complexes **2** and **3** to form a distorted tetrahedral geometry. Complex **5** has only one triphenylphosphine coordinated to the copper(I) center with a nitrate ion coordinated to the same metal center through oxygen atom to adopt a distorted tetrahedral geometry. All complexes synthesized exhibited strong antimicrobial activity almost two-fold the strength of the ancillary and free ligands suggestive of the mutually inclusive synergy of triphenyphosphine and pyridnyl Schiff base ligands in the complexes formed pointing to the potentials of the complexes as plausible antibacterial agents.

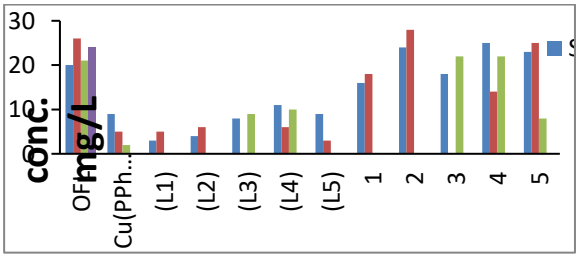

Figure 3.5: Inhibitory activity of uncomplexed Schiff base ligands **L1-L5** , ancillary ligand (PPh_3) and respective Cu(I) complexes **1-5** .

References

Adeleke, A. A., Islam, M. S., Sanni, O., Mocktar, C., Zamisa, S. J., & Omondi, B. (2021). Aryl variation and anion effect on CT-DNA binding and in vitro biological studies of pyridinyl Ag (I) complexes. *Journal of Inorganic Biochemistry, 214*, 111266.

Adeleke, A. A., Islam, M. S., Omondi, B. (2023). Silver(I) pyridinyl complexes with benzothiazole, thiophene, and furan moieties: DNA/protein-binding, antibacterial, antioxidant, and anticancer studies. *Arch Pharm (Weinheim), 356*, e2200308. doi:10.1002/ardp.202200308

Adeleke, A. A., Zamisa, S. J., Islam, Md. S., Olofinsan, K., Salau, V. F., Mocktar, C., Omondi, B. (2021). Quinoline Functionalized Schiff Base Silver (I) Complexes: Interactions with Biomolecules and In Vitro Cytotoxicity, Antioxidant and Antimicrobial Activities. *Molecules, 26*(5), 1205.

Adeleke, A. A., Zamisa, S. J., Omondi, B. (2020). Crystal structure of dichlorido-bis((E)-2-((pyridin-4-ylmethylene)amino)phenol)zinc(II), $C_{24}H_{20}Cl_2N_4O_2Zn$. *Z. Kristallogr. NCS, 235*(3), 625-628. doi:10.1515/ncrs-2019-0863

Andruh, M. (2015). The exceptionally rich coordination chemistry generated by Schiff-base ligands derived from o-vanillin. *Dalton Transactions, 44*(38), 16633-16653.

Cross, E. D., Ang, M. T. C., Richards, D. D., Clemens, A. C., Muthukumar, H., McDonald, R., Woodfolk, L., Ckless, K., & Bierenstiel, M. (2018). Synthesis, characterization, cytotoxicity and antimicrobial activity of copper complexes of N-imine pendant derivatives of 2-(methylthio) aniline. *Inorganica Chimica Acta*, *481*, 69-78.

Dharmaraj, N., Viswanathamurthi, P., & Natarajan, K. (2001). Ruthenium (II) complexes containing bidentate Schiff bases and their antifungal activity. *Transition metal chemistry, 26*(1), 105-109.

Farrugia, L. J. (2012). WinGX and ORTEP for Windows: an update. *Journal of applied crystallography, 45*(4), 849-854.

Griebel, C., Hodges, D. D., Yager, B. R., Liu, F. L., Zhou, W., Karavage, K. J., Zhu, Y., Norman, S. G., Lan, R., & Day, C. S. (2020). Bisbiphenyl Phosphines: Structure and Synthesis of Gold (I) Alkene π-Complexes with Variable Phosphine Donicity and Enhanced Stability. *Organometallics, 39*(14), 2665-2671.

Karlin, K. D., Cohen, B. I., Hayes, J. C., Farooq, A., Zubieta, J. (1987). Models for methemocyanin derivatives: structural and spectroscopic comparisons of related azido-coordinated (N3-) mono-and dinuclear copper (II) complexes. *Inorganic Chemistry, 26*(1), 147-153.

Karp, J., Botana, A. S., Norman, M. R., Park, H., Zingl, M., & Millis, A. (2020). Many-body electronic structure of NdNiO 2 and CaCuO 2. *Physical Review X, 10*(2), 021061.

Lobana, T. S., Bhatia, P. K., & Tiekink, E. R. T. (1989). Synthesis and X-ray crystal structure of chloro [2 (1 H)-pyridinethione-S]-bis (triphenylphosphine) copper (I). *Journal of the Chemical Society, Dalton Transactions*(4), 749-751.

Marston, H. D., Dixon, D. M., Knisely, J. M., Palmore, T. N., & Fauci, A. S. (2016). Antimicrobial resistance. *Jama, 316*(11), 1193-1204.

Morse, S. S. (2001). Factors in the emergence of infectious diseases. *Plagues and politics*, 8-26.

Njogu, E. M., Nyamori, V. O., & Omondi, B. (2017). Coordination polymers and

discrete complexes of Ag (I)-N-(pyridylmethylene) anilines: Synthesis, crystal structures and photophysical properties. *Journal of Coordination Chemistry, 70*(16), 2796-2814.

Njogu, E. M., Omondi, B., Nyamori, V. O. (2018). Crystal structure of aqua-bis {[2, 6-dimethyl-N-(pyridin-2-ylmethylene) aniline-κ2N, N′]} zinc (II) triflate monohydrate [ZnC29H31N4O] CF3SO3· H2O. *Zeitschrift für Kristallographie-New Crystal Structures, 233*(1), 7-8.

Oladipo, S. D., & Mocktar, C. (2019). Synthesis and structural studies of nickel (II)-and copper (II)-N, N′-diarylformamidine dithiocarbamate complexes as antimicrobial and antioxidant agents. *Polyhedron, 170*, 712-722.

Pettinari, C., Tăbăcaru, A., & Galli, S. (2016). Coordination polymers and metal–organic frameworks based on poly (pyrazole)-containing ligands. *Coordination Chemistry Reviews, 307*, 1-31.

Raj, P., Singh, A., Singh, A., & Singh, N. (2017). Syntheses and photophysical properties of Schiff base Ni (II) complexes: application for sustainable antibacterial activity and cytotoxicity. *ACS Sustainable Chemistry & Engineering, 5*(7), 6070-6080.

Ramachandran, E., Raja, D. S., Bhuvanesh, N. S. P., & Natarajan, K. (2012). Mixed ligand palladium (II) complexes of 6-methoxy-2-oxo-1, 2-dihydroquinoline-3-carbaldehyde 4 N-substituted thiosemicarbazones with triphenylphosphine co-ligand: synthesis, crystal structure and biological properties. *Dalton Transactions, 41*(43), 13308-13323.

Raman, N., Sakthivel, A., & Jeyamurugan, R. (2009). Synthesis, characterization, DNA binding, photo-induced DNA cleavage, and antimicrobial activity of metal complexes of a Schiff base derived from bis (3-aminophenyl) malonamide. *Journal of Coordination Chemistry, 62*(24), 3969-3985.

Ribeiro, N., Roy, S., Butenko, N., Cavaco, I., Pinheiro, T., lho, I., Marques, F., Avecilla, F., Pessoa, J. C., & Correia, I. (2017). New Cu (II) complexes with pyrazolyl derived Schiff base ligands: Synthesis and biological evaluation. *Journal of Inorganic Biochemistry, 174*, 63-75.

Santini, C., Pellei, M., Lobbia, G. G., Cingolani, A., Spagna, R., & Camalli, M. (2002). Unprecedented phosphino copper (I) derivatives of tris (pyrazolyl) methanesulfonate ligand co-ordinated to metal in an unusual κ3-N, N′, O fashion. *Inorganic Chemistry Communications, 5*(6), 430-433.

Schnödt, J., Manzur, J., García, A. M., Hartenbach, I., Su, C. Y., Fiedler, J., & Kaim, W. (2011). Coordination of a Hemilabile N, N, S Donor Ligand in the Redox System [CuL2]+/2+, L= 2-Pyridyl-N-(2′-alkylthiophenyl) methyleneimine: Wiley Online Library.

Shabbir, M., Akhter, Z., Ahmad, I., Ahmed, S., Shafiq, M., Mirza, B., McKee, V., Munawar, K. S., & Ashraf, A. R. (2016). Schiff base triphenylphosphine palladium (II) complexes: Synthesis, structural elucidation, electrochemical and biological evaluation. *Journal of Molecular Structure, 1118*, 250-258.

Sheldrick, G. M. (2008). A short history of SHELX. *Acta Crystallographica Section A: Foundations of Crystallography, 64*(1), 112-122.

Sheldrick, G. M. (2015). Crystal structure refinement with SHELXL. *Acta Crystallographica Section C: Structural Chemistry, 71*(1), 3-8.

Simkhovich, L., Galili, N., Saltsman, I., Goldberg, I., Gross, Z.,. (2000). Coordination chemistry of the novel 5, 10, 15-tris (pentafluorophenyl) corrole: Synthesis, spectroscopy, and structural characterization of its cobalt (III), rhodium (III), and iron (IV) complexes. *Inorganic Chemistry, 39*(13), 2704-2705.

Sun, X. Z., Yan, H. J., Wan, C. Q. (2013). Crystal structure of poly [μ2-di-4-pyridinylmethanone-κ2N: N'-silver (I)] trifluoroacetate-water-acetonitrile (2/1/1), C14H10. 5AgF3N2. 50O3. 50. *Zeitschrift für Kristallographie-New Crystal Structures, 228*(3), 375-376.

Vijayan, P., Viswanathamurthi, P., Silambarasan, V., Velmurugan, D., Velmurugan, K.,

Nandhakumar, R., Butcher, R. J., Silambarasan, T., & Dhandapani, R. (2014). Dissymmetric thiosemicarbazone ligands containing substituted aldehyde arm and their ruthenium (II) carbonyl complexes with PPh3/AsPh3 as ancillary ligands: Synthesis, structural characterization, DNA/BSA interaction and in vitro anticancer activity. *Journal of Organometallic Chemistry, 768*, 163-177.

Viswanathamurthi, P., Karvembu, R., Tharaneeswaran, V., & Natarajan, K. (2005). Ruthenium (II) complexes containing bidentate Schiff bases and triphenylphosphine or triphenylarsine. *Journal of Chemical sciences, 117*(3), 235-238.

Yang, L., Powell, D. R., & Houser, R. P. (2007). Structural variation in copper (I) complexes with pyridylmethylamide ligands: structural analysis with a new four-coordinate geometry index, τ 4. *Dalton Transactions*(9), 955-964.

Zheng, D., Huang, T.-H., Luo, C., & Tang, J. (2022a). Structural characterization, DFT studies and luminescent properties of dinuclear copper (I)-diimine complexes with the S-shape configurations. *Inorganica Chimica Acta*, *529*, 120639.

Zheng, D., Huang, T. H., Luo, C., & Tang, J. (2022b). Structural characterization, DFT studies and luminescent properties of dinuclear copper (I)-diimine complexes with the S-shape configurations. *Inorganica Chimica Acta, 529*, 120639.